Original Paper

Integrating Multidimensional Clinical Data to Develop a Visual Nomogram for Individualized Prediction of Postinfectious Bone Loss in Patients With Spinal Infection: Retrospective Cohort Study

Xi Chen[1*], MD; Shouxiang Kuang[1*], MD; Rongpan Dang[2], PhD; Yang Li[1], PhD; Guodong Wang[1], PhD; Jianmin Sun[2], PhD; Fengge Zhou[1], PhD; Hongdong Tan[2], PhD; Chenggui Zhang[1*], PhD

[1]Shandong Provincial Hospital Affiliated to Shandong First Medical University, Jinan, Shandong, China

[2]Shandong Public Health Clinical Center, Shandong University, Jinan, China

[*]these authors contributed equally

Corresponding Author:
Chenggui Zhang, PhD
Shandong Provincial Hospital Affiliated to Shandong First Medical University
Department of Orthopaedics
No. 324, Jingwu Weiqi Road, Huaiyin District
Jinan, Shandong, 250021
China
Phone: 86 18810169013
Email: chenggui1214@pku.edu.cn

Abstract

Background: Postinfectious bone loss can lead to spinal instability and severe neurological complications, with potentially devastating outcomes. However, prognostic models to support individualized risk assessment remain limited.

Objective: This study aimed to develop and internally validate a visual nomogram integrating multimodal clinical data to estimate postinfectious bone loss risk in patients with spinal infection and inform individualized monitoring strategies.

Methods: This retrospective cohort study used consecutive sampling at Shandong Public Health Clinical Center. Baseline clinical and laboratory data were extracted from medical records. Eligible patients had confirmed spinal infection, a baseline vertebral bone destruction height ratio less than one-third, and complete baseline and follow-up data. Postinfectious bone loss was defined as a height ratio greater than or equal to one-third on computed tomography 12 months after baseline. Predictors were selected from 31 baseline variables using univariable logistic regression followed by least absolute shrinkage and selection operator (LASSO) regression. Multivariable logistic regression was used to construct the nomogram. Internal validation used 500 bootstrap resamples, repeating all predictor selection and model-fitting steps. Performance was assessed using the area under the receiver operating characteristic curve (AUC), calibration curves, the Brier score, decision curve analysis, and clinical impact curve analysis.

Results: Postinfectious bone loss occurred in 48.9% (109/223, 95% CI 42.4%-55.4%) of patients. The nomogram combined infection characteristics (multidrug-resistant bacterial infection and infected spinal segment), skeletal status (osteoporosis), and laboratory markers (interleukin-6, albumin, and plasma fibrinogen) to estimate individual risk. In the multivariable model, the odds ratios (ORs) were 2.718 (95% CI 0.993-7.444; *P*=.05) for multidrug-resistant bacterial infection and 7.345 (95% CI 2.757-19.570; *P*<.001) for osteoporosis. Relative to cervical infection, ORs were 14.041 (95% CI 1.079-182.662; *P*=.04) for thoracic, 28.876 (95% CI 2.648-314.895; *P*=.006) for lumbar, and 12.604 (95% CI 0.436-364.075; *P*=.14) for thoracolumbar infection. Per unit increase, ORs were 1.004 (95% CI 0.996-1.012; *P*=.30) for interleukin-6 (pg/mL), 3.673 (95% CI 2.410-5.598; *P*<.001) for plasma fibrinogen (g/L), and 0.834 (95% CI 0.749-0.929; *P*=.001) for albumin (g/L). Discrimination remained high after optimism correction, with an AUC of 0.946 (95% CI 0.919-0.972), compared with an apparent AUC of 0.954 (95% CI 0.931-0.978). Calibration assessment yielded an intercept of 0.00 (95% CI –0.43 to 0.43) and a slope of 1.00 (95% CI 0.75-1.25), while the Brier score was 0.096 (95% CI 0.064-0.118), indicating close agreement between predicted and observed risks and low overall prediction error.

Conclusions: This study developed a visual nomogram integrating baseline clinical characteristics, imaging features, and laboratory parameters to predict postinfectious bone loss in patients with spinal infection. Extending previous association studies

XSL•FO
RenderX

to individualized risk prediction, the model showed good discrimination and calibration in internal validation. This approach may help identify high-risk patients and inform closer monitoring and timely reassessment before further structural deterioration and neurological complications.

(J Med Internet Res 2026;28:e93326) doi: 10.2196/93326

KEYWORDS

nomograms; postinfectious bone loss; prediction model; risk assessment; spinal infection

Introduction

Problem

Spinal infection remains a serious clinical and public health challenge, with increasing incidence and growing demands on clinical services [1]. Delayed diagnosis, heterogeneous microbial etiologies, and complex treatment requirements further complicate its management [2]. Treatment requires both infection control and efforts to limit secondary vertebral destruction [3]. Experimental evidence demonstrates that infection can stimulate osteoclast-mediated bone resorption, contributing to bone loss [4]. Progressive vertebral destruction can compromise spinal stability and lead to deformity and neurological impairment, including paralysis [5]. Structural deterioration may continue during conservative treatment [6], and severe vertebral destruction has been associated with increased mortality [7]. These consequences emphasize the importance of identifying patients at risk of further bone loss early in the course of treatment.

However, recent studies of vertebral damage have mainly examined associated factors or quantified bone loss already present [8]. Existing prediction models have addressed inadequate treatment response in vertebral osteomyelitis [9] and postoperative bone nonunion in infectious spondylitis [10]. These outcomes differ from subsequent infection-related bone loss and do not directly address individualized prediction of this structural complication. Evidence supporting quantitative prediction of postinfectious bone loss therefore remains limited. A model specifically targeting this outcome is needed to provide individualized risk estimates.

Review of Relevant Scholarship

Vertebral bone destruction is a serious complication of spinal infection that may compromise spinal stability, cause severe neurological impairment, including paralysis, and necessitate surgical intervention; severe destruction has also been associated with increased mortality [7]. However, existing prediction models for spinal infection have primarily focused on inadequate treatment response, postoperative nonunion, and mortality [9-11]. Studies addressing spinal infection-related vertebral bone loss and destruction have largely relied on analyses of associated factors, spinal instability scoring systems, and imaging-based regression models. These approaches nevertheless have limitations in predicting the subsequent progression of vertebral bone destruction.

Specifically, Hockmann et al [7] developed a model to assess the severity of existing vertebral destruction in patients with spinal infection but did not report model calibration or undertake internal or external validation. The modified Spinal Instability Spondylodiscitis Score was primarily designed to assess and classify infection-related spinal instability, with validation focusing mainly on interrater agreement rather than the prediction of subsequent clinical outcomes [12]. Similarly, Lang et al [8] developed an imaging-based regression model to quantify existing vertebral bone loss in a small retrospective cohort but did not further evaluate its ability to predict subsequent progression of vertebral destruction. Although previous studies have assessed vertebral destruction in spinal infection, they mainly focused on existing damage. Evidence on model calibration and validation was also limited. A new model is therefore needed to predict individual risk of postinfectious bone loss using data available at initial diagnosis.

Notably, a nomogram is a graphical representation of a multivariable prediction model that assigns points to individual predictors and translates the total score into an estimated probability of an outcome, thereby enabling individualized risk prediction [13].

Currently, several prediction models have been developed to assess adverse outcomes and treatment-related complications in patients with spinal infection, including poor treatment response, postoperative nonunion, and mortality. Li et al [9] developed a nomogram to predict the risk of poor treatment response in patients with vertebral osteomyelitis. Zhao et al [10] established a prediction model for nonunion following instrumented spinal fusion in patients with infectious spondylitis, focusing primarily on postoperative fusion outcomes. In addition, another study by Li et al [11] developed a nomogram to predict 1-year mortality in patients with vertebral osteomyelitis, with an emphasis on survival prognosis. However, studies specifically focusing on vertebral bone loss associated with spinal infection remain limited.

Hypothesis, Aims, and Objectives

This study aimed to develop and internally validate a nomogram for predicting postinfectious bone loss in patients with spinal infection. The nomogram was designed to combine baseline data, including clinical characteristics, laboratory findings, microbiological data, and imaging features, for risk assessment at initial diagnosis.

Methods

Inclusion and Exclusion

The inclusion criteria were as follows: (1) spinal infection was confirmed by pathogen identification in biopsy specimens [14]; (2) the vertebral bone destruction height ratio was less than one-third on baseline computed tomography (CT); (3) CT images obtained 12 months after baseline were available for

XSL•FO
RenderX

outcome assessment; and (4) complete baseline data were available, including clinical, laboratory, microbiological, and imaging records.

The exclusion criteria were as follows: (1) patients had noninfectious bone disease, such as osteoporotic fractures; (2) the causative pathogen could not be identified; (3) required data were missing or incomplete, including demographic and clinical information, laboratory results, microbiological findings, imaging findings, bone mineral density measurements, or follow-up CT data; and (4) the vertebral bone destruction height ratio was greater than or equal to one-third on baseline CT.

Participant Characteristics

The study included patients with confirmed spinal infection treated in the Department of Spinal Infection Surgery at Shandong Public Health Clinical Center. Baseline information comprised demographic and clinical characteristics, microbiological findings, laboratory measurements, imaging data, and osteoporosis status.

Sampling Procedures

This study used consecutive sampling. The medical records of 436 patients were reviewed retrospectively to identify eligible patients according to the prespecified inclusion and exclusion criteria.

Sample Size, Power, and Precision

The sample size was determined by the number of eligible patients with complete records during the study period. Sample size, statistical power, and precision were not calculated in advance. To describe the number of outcome events relative to the complexity of the final model, we calculated the events per predictor parameter (EPP) ratio by dividing the number of outcome events by the number of predictor parameters in the final model, excluding the intercept [15].

Measures and Covariates

Outcome Definition and Assessment

The study outcome was postinfectious bone loss, assessed using archived CT images obtained 12 months after the initial diagnostic assessment (baseline). With reference to previous CT-based measurement methods [16], the vertebral bone destruction height ratio was calculated on reconstructed sagittal CT images by dividing the height of the bone destruction area by the normal vertebral body height. The height ratio was measured on the midsagittal CT slice and on 2 additional sagittal slices. One slice was located a quarter of the vertebral body width inward from the left lateral margin, and the other was located the same distance inward from the right lateral margin. The 3 height ratios were averaged. For multilevel infection, each affected spinal unit was assessed separately, and the highest mean ratio was used [16]. Previous CT-based grading criteria used a threshold of one-third to distinguish between limited vertebral destruction and more extensive destruction [17]. Based on these criteria, a height ratio greater than or equal to one-third at 12 months was prespecified before model development as the criterion for postinfectious bone loss, which served as the binary study outcome. All included patients had baseline height ratios below this threshold, and the same measurement procedure was applied at both time points. The schematic illustration of the measurement is provided in Figure S1 in Multimedia Appendix 1.

Candidate Predictors and Covariates

Baseline candidate predictors were specified before statistical screening based on clinical plausibility, clinical experience, and published reviews of spinal infection [18]. Demographic variables included age and sex. Clinical manifestations included pain, fever, and neurological impairment. Comorbidities included hypertension, diabetes, liver disease, kidney disease, cardiovascular disease, cerebrovascular disease, pneumonia, and osteoporosis. Symptoms and comorbidities were recorded according to documented clinical assessments. Osteoporosis was assessed from baseline dual-energy X-ray absorptiometry (DXA) reports and clinical diagnoses. In postmenopausal women and men aged 50 years or older, a T-score of less than or equal to –2.5 at the lumbar spine, total hip, or femoral neck met the densitometric criterion [19]. All predictors were assessed at baseline, before the defined outcome occurred.

The causative pathogens were grouped into 5 categories: gram-positive cocci, gram-negative bacilli, *Mycobacterium tuberculosis*, *Brucella* species, and fungi. The identified bacteria were further assessed for multidrug resistance. For bacterial species covered by the international consensus criteria, multidrug resistance was defined as acquired nonsusceptibility to at least 1 agent in 3 or more antimicrobial categories [20].

Laboratory variables were grouped into 4 categories. Hematological parameters included white blood cell count, red blood cell count, hemoglobin, and platelet count. Inflammatory markers included C-reactive protein, erythrocyte sedimentation rate, and interleukin-6 (IL-6). The biochemical marker was albumin. Coagulation-related parameters included activated partial thromboplastin time, plasma fibrinogen, thrombin time, and D-dimer. These measurements were analyzed as continuous predictors.

Imaging variables included the infected spinal segment, number of infected vertebrae, localized kyphosis, and epidural abscess.

The infected spinal segment was classified as cervical, thoracic, lumbar, or thoracolumbar. The number of infected vertebrae was defined as the total count of vertebral bodies showing characteristic infectious changes on CT, including endplate erosion, vertebral destruction, or contrast enhancement, and was categorized as 1, 2, or greater than or equal to 3 [21,22]. Localized kyphosis was assessed using the Cobb method [23], with the angle measured between the superior endplate of the uppermost affected vertebra and the inferior endplate of the lowermost affected vertebra on reconstructed midsagittal CT images. A Cobb angle of greater than 20° was used as the study-specific criterion for localized kyphosis. Epidural abscess was defined as a focal collection within the epidural space adjacent to the infected vertebrae, exhibiting low T1-weighted and high T2-weighted signal intensity on baseline magnetic resonance imaging (MRI) [6].

XSL•FO
RenderX

Data Collection

Data were retrospectively extracted from the hospital's electronic medical records, laboratory and microbiology reports, DXA reports, and archived CT and MRI examinations. Demographic and clinical data were obtained from clinical records. Clinical data included symptoms and comorbidities. Laboratory values were taken directly from the initial test reports. Pathogen identification and antimicrobial susceptibility results were obtained from the biopsy workup performed during the initial diagnostic assessment.

Quality of Measurements

Two experienced surgeons independently reviewed the archived imaging data and relevant clinical records under blinded conditions using predefined assessment criteria. Disagreements were adjudicated by a third senior reviewer to establish the final classifications.

Masking

Participant masking was not applicable because this was a retrospective study. During independent assessment of baseline CT images and CT images obtained at the time of outcome assessment, the 2 reviewers were blinded to clinical and laboratory information. They were provided only with CT images. Masking was evaluated through checks of the supplied imaging materials and questionnaires completed by both reviewers. No breaches of masking were identified from the material checks or questionnaire responses.

Psychometrics

Interobserver agreement was calculated from the initial independent assessments before adjudication. Cohen κ coefficients were used for binary variables, including postinfectious bone loss, localized kyphosis, and epidural abscess, and for the nominal categorical variable of infected spinal segment [24]. Weighted κ was used for the categorized number of infected vertebrae (1, 2, or ≥3), an ordinal variable [25]. All κ estimates were reported with their corresponding 95% CIs (Table S1 in Multimedia Appendix 1).

Agreement was interpreted according to the criteria by Landis and Koch [26]: κ values of 0.00 to 0.20 indicated slight agreement, 0.21 to 0.40 fair agreement, 0.41 to 0.60 moderate agreement, 0.61 to 0.80 substantial agreement, and 0.81 to 1.00 almost perfect agreement.

Conditions and Design

This study used a nonexperimental, observational, retrospective cohort design. No intervention was assigned by the research team, and no experimental manipulation or random allocation was involved. The study was conducted at the Department of Spinal Infection Surgery, Shandong Public Health Clinical Center, China, among patients with confirmed spinal infection evaluated between January 1, 2023, and December 31, 2024.

Data Diagnostics

The extracted medical record data were checked for completeness, logical consistency, coding accuracy, and consistency of measurement units. The distributions of continuous variables were examined using descriptive statistics, and normality was assessed using the Shapiro-Wilk test. Identified transcription errors and unit inconsistencies were corrected by referring to the original laboratory reports. All 223 eligible patients were included in the final analysis.

The final dataset contained complete data for all 31 candidate predictors and the CT outcome. Therefore, no imputation was required, and the missing completely at random (MCAR) test by Little was not applicable. Continuous predictors were entered into the final logistic regression model on their original measurement scales.

Analytic Strategy

The primary hypothesis was that specific baseline clinical, laboratory, microbiological, imaging, and other variables were associated with postinfectious bone loss in patients with spinal infection. To identify potential predictors, the 31 baseline candidate variables were screened using univariable logistic regression. Variables with $P \leq .20$ were further selected using least absolute shrinkage and selection operator (LASSO) regression with 5-fold cross-validation and the 1 SE rule. The retained predictors were entered into a multivariable logistic regression model to estimate adjusted odds ratios (ORs) with 95% CIs.

The secondary hypothesis was that a multivariable prediction model incorporating the selected baseline predictors could accurately estimate the risk of postinfectious bone loss. A nomogram was developed based on the final multivariable logistic regression model. Model discrimination was assessed using the area under the receiver operating characteristic curve (AUC), while calibration was evaluated using calibration curves, the calibration intercept, calibration slope, and Brier score. Internal validation was performed using 500 bootstrap resamples, with the entire variable selection and model-fitting process repeated within each resample to obtain optimism-corrected estimates of predictive performance.

The exploratory hypothesis was that the developed nomogram could provide useful information for clinical risk stratification and individualized decision-making. Decision curve analysis (DCA) was performed to assess the model's potential clinical net benefit across a range of risk thresholds, compared with treat-all and treat-none strategies. Clinical impact curve (CIC) analysis was used to illustrate the number of patients classified as high risk and the number among them who experienced postinfectious bone loss at different risk thresholds. These analyses were intended to explore the model's potential clinical utility rather than establish its effectiveness in improving patient outcomes.

The analyses were primarily intended for predictor identification, model development, and exploratory assessment of clinical utility rather than confirmatory testing of multiple independent hypotheses. *P* values from univariable logistic regression were used for preliminary predictor screening and were not interpreted as confirmatory evidence of independent associations. LASSO regression with cross-validation was used to limit model complexity, while bootstrap internal validation was performed to assess potential overfitting and optimism. No formal adjustment for multiple comparisons was applied. All

XSL•FO
RenderX

statistical tests were 2-sided, with a nominal significance threshold of $P<.05$.

Statistical Analysis

The study was reported in accordance with the TRIPOD (Transparent Reporting of a Multivariable Prediction Model for Individual Prognosis or Diagnosis) statement [27]. Statistical analyses were performed using the Free Statistics Analysis Platform (version 2.2) and R software (version 4.2.2; R Foundation for Statistical Computing). Continuous variables were assessed for normality using the Shapiro-Wilk test. Normally distributed variables were summarized as mean (SD) and compared between patients with and without postinfectious bone loss using independent-samples *t* tests. Nonnormally distributed variables were summarized as median (IQR) and compared using Mann-Whitney *U* tests. Categorical variables were presented as counts and percentages. Nominal variables were compared using chi-square tests or Fisher exact tests, whereas ordinal variables were compared using Mann-Whitney *U* tests. All statistical tests were 2-sided, with a significance level of $\alpha=.05$.

Given the large number of candidate predictors and the relatively limited sample size, the 31 baseline candidate predictors were initially screened using univariable logistic regression to reduce the candidate set and control model complexity. This analytical strategy is consistent with approaches used in comparable clinical nomogram studies [9,10,28,29]. A relatively liberal threshold of $P\leq.20$ was used to retain variables with modest individual associations for further assessment. Variables meeting this criterion were included in a LASSO logistic regression model fitted using the *glmnet* R package (version 4.1-8 [30]). The penalty parameter (λ) was selected using 5-fold cross-validation. The 1 SE rule ($\lambda_1$se) was used to favor a simpler model [30]. Predictors with nonzero coefficients at the selected λ were retained for multivariable modeling.

The retained predictors were entered jointly into a multivariable logistic regression model. Categorical predictors were coded as indicator variables, and continuous predictors were analyzed on their original scales. Adjusted ORs were reported with 95% CIs, and *P* values were calculated using Wald tests. Coefficient extraction and formatting were supported by the *broom* (version 1.0.5) and *dplyr* (version 1.1.4) packages. Multicollinearity among predictors in the final model was assessed using generalized variance inflation factors (GVIFs), adjusted for predictor degrees of freedom, with $GVIF^{1/(2\times df)}$ calculated to account for differences in predictor degrees of freedom [31]. Restricted cubic splines (RCSs) were used to assess the linearity of continuous predictors on the log-odds scale [32]. The final model was presented as a nomogram using the *rms* package (version 6.7-1).

Apparent model performance was evaluated in the full cohort. Discrimination was assessed using the *pROC* package (version 1.18.4) to generate receiver operating characteristic (ROC) curves and calculate the AUC. The optimal predicted probability threshold was determined by maximizing the Youden index (sensitivity + specificity – 1). Sensitivity and specificity were calculated at this threshold. Calibration was assessed using calibration curves, the calibration intercept, and the calibration slope calculated with the rms package. Overall prediction error was assessed using the Brier score. This score was calculated as the mean squared difference between predicted probabilities and observed outcomes [33].

Internal validation was performed to estimate and correct optimism in model performance. We generated 500 bootstrap samples by sampling with replacement from the full cohort. Each sample contained the same number of patients as the original cohort. Univariable screening, LASSO tuning and predictor selection, and multivariable logistic regression fitting were repeated within each resample. Each resulting model was evaluated in both its bootstrap sample and the original cohort. For each performance measure, we subtracted the original-cohort estimate from the bootstrap-sample estimate. These differences were averaged across resamples. The average difference was then subtracted from the original model's apparent performance to obtain the optimism-corrected estimate [34].

Potential clinical utility was assessed using exploratory DCA. The model's net benefit was compared with those of the treat-all and treat-none strategies across a range of threshold probabilities [35]. CIC analysis was used to describe high-risk patient classification at each threshold. Patients were classified as high risk when their predicted probability met or exceeded the threshold. The curves showed the total number of patients classified as high risk and the number of these patients who developed postinfectious bone loss. Both counts were expressed per 100 patients [36]. The *ggplot2* package (version 3.4.4) was used for graphical visualization.

Ethical Considerations

This retrospective study was approved by the Ethics Committee of Shandong Public Health Clinical Center (approval number gwlczxec-SOP-K-2025-137) and conducted in accordance with the Declaration of Helsinki. Given the retrospective design and use of anonymized patient data, the committee waived the requirement for informed consent. The research dataset contained no personal identifiers. No compensation was provided to participants. The manuscript and supplementary materials contained no identifiable patient information or images.

Results

Participant Flow and Baseline Characteristics

A total of 436 patient records were screened for eligibility. Of these, 64 were excluded because needle biopsy had not been performed. Among the remaining 372 patients, 149 were excluded because of noninfectious bone disease (n=43), an unidentified causative pathogen (n=44), incomplete key diagnostic or clinical data (n=30), or a baseline vertebral bone destruction ratio greater than or equal to one-third (n=32). The remaining 223 patients were included in the final cohort. All included patients had a baseline vertebral bone destruction ratio less than one-third and complete baseline and 12-month outcome data.

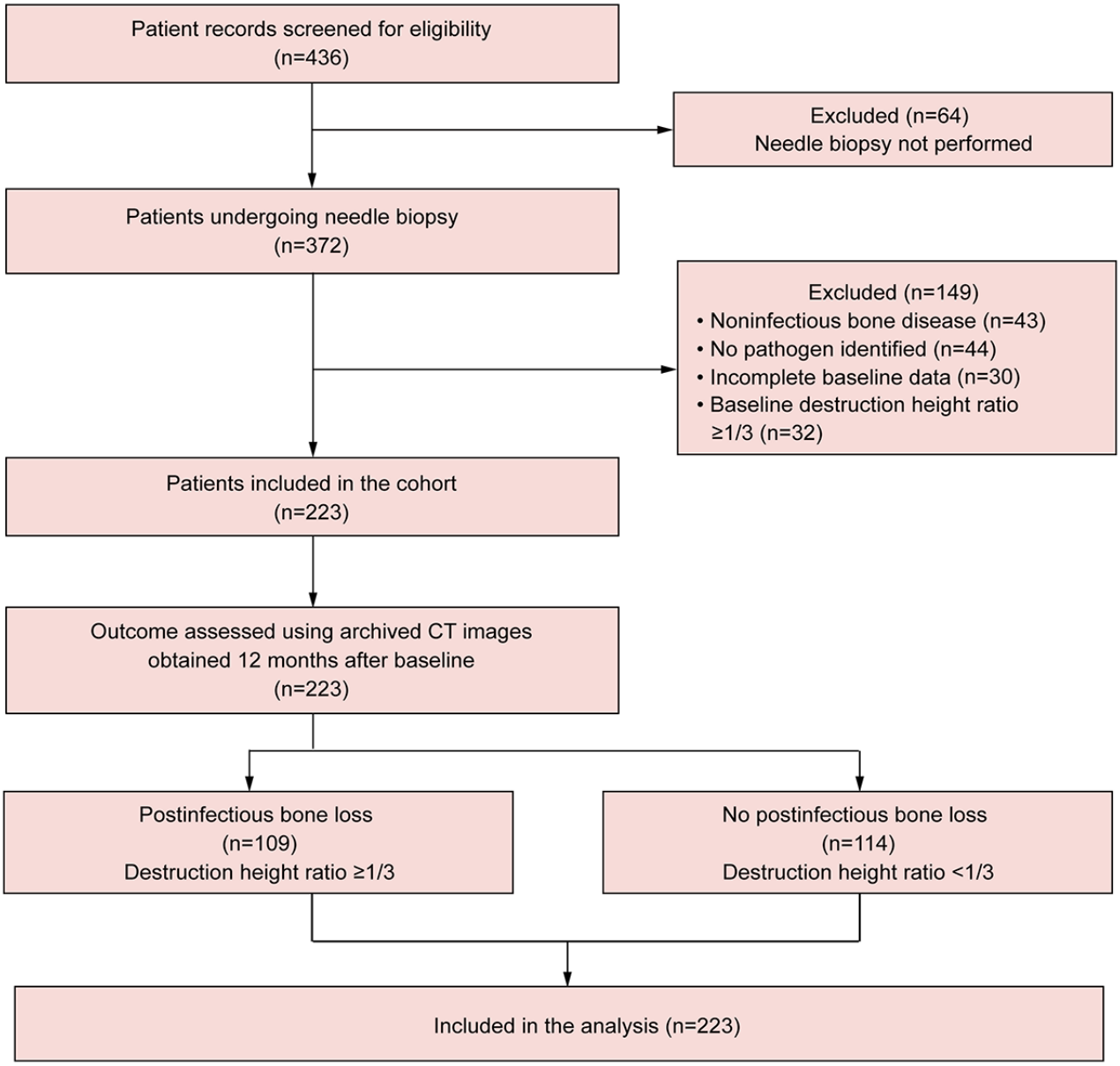
Among the 223 patients, 109 (48.9%, 95% CI 42.4%-55.4%) developed postinfectious bone loss at 12 months, whereas 114

XSL•FO
RenderX

(51.1%, 95% CI 44.6%-57.6%) did not. All 223 patients were included in model development and internal validation. The participant flow and reasons for exclusion are shown in Figure 1.

Baseline characteristics and comparisons between the outcome groups are summarized in Table 1. The mean age was 60.2 (SD 15.3) years; 84 patients were men and 139 were women. Age (*P*=.66) and sex (*P*=.42) did not differ significantly between patients with and without postinfectious bone loss. Infection with multidrug-resistant bacteria was more frequent among patients with bone loss than among those without bone loss (49/109 vs 34/114; *P*=.02), as was osteoporosis (81/109 vs 35/114; *P*<.001). The groups also differed in the distributions of pathogen categories (*P*=.048) and infected spinal segments (*P*=.005). Median IL-6 was 33.1 (IQR 13.5-124.7) pg/mL in the bone loss group and 21.5 (IQR 9.3-38.6) pg/mL in the group without bone loss (*P*=.005). Mean plasma fibrinogen was higher in the bone loss group, at 6.4 (SD 1.1) g/L compared with 3.9 (SD 1.5; *P*<.001) g/L. Mean albumin was lower, at 33.2 (SD 4.1) g/L compared with 37.3 (SD 4.4; *P*<.001) g/L.

Figure 1. Flowchart of the procedure. A total of 436 patient records from Shandong Public Health Clinical Center from January 1, 2023, to December 31, 2024, were screened for eligibility. After exclusions, 223 patients with confirmed spinal infection and a baseline vertebral bone destruction ratio less than one-third were included. Outcomes were assessed using archived computed tomography (CT) images obtained 12 months after baseline; 109 patients developed postinfectious bone loss and 114 did not. The full cohort was used for nomogram development and internal validation using 500 bootstrap resamples.



XSL•FO
RenderX

Table 1. Demographic and clinical characteristics of the study cohort.

Characteristics	Total (n=223)	No bone loss (n=114)	Bone loss (n=109)	*P* value
MDRB[a] , n (%)				.02
No	140 (62.8)	80 (70.2)	60 (55)	
Yes	83 (37.2)	34 (29.8)	49 (45)	
Pathogen type, n (%)				.048
Gram-positive cocci	101 (45.3)	53 (46.5)	48 (44)	
Gram-negative bacilli	66 (29.6)	32 (28.1)	34 (31.2)	
Mycobacterium tuberculosis	32 (14.3)	12 (10.5)	20 (18.3)	
Brucella species	19 (8.5)	15 (13.2)	4 (3.7)	
Fungi	5 (2.2)	2 (1.8)	3 (2.8)	
Age (years)				.66
Mean (SD)	60.2 (15.3)	60.6 (15.6)	59.7 (15.0)	
Sex, n (%)				.42
Male	84 (37.7)	40 (35.1)	44 (40.4)	
Female	139 (62.3)	74 (64.9)	65 (59.6)	
Pain, n (%)				.16
No	24 (10.8)	9 (7.9)	15 (13.8)	
Yes	199 (89.2)	105 (92.1)	94 (86.2)	
Fever, n (%)				.61
No	165 (74.0)	86 (75.4)	79 (72.5)	
Yes	58 (26.0)	28 (24.6)	30 (27.5)	
Neurological impairment, n (%)				.91
No	199 (89.2)	102 (89.5)	97 (89)	
Yes	24 (10.8)	12 (10.5)	12 (11)	
Hypertension, n (%)				.59
No	183 (82.1)	92 (80.7)	91 (83.5)	
Yes	40 (17.9)	22 (19.3)	18 (16.5)	
Diabetes, n (%)				.87
No	181 (81.2)	93 (81.6)	88 (80.7)	
Yes	42 (18.8)	21 (18.4)	21 (19.3)	
Hepatopathy, n (%)				.68
No	217 (97.3)	110 (96.5)	107 (98.2)	
Yes	6 (2.7)	4 (3.5)	2 (1.8)	
Kidney disease, n (%)				.72
No	215 (96.4)	109 (95.6)	106 (97.2)	
Yes	8 (3.6)	5 (4.4)	3 (2.8)	
Cardiovascular disease, n (%)				.88
No	206 (92.4)	105 (92.1)	101 (92.7)	
Yes	17 (7.6)	9 (7.9)	8 (7.3)	
Cerebrovascular disease, n (%)				.91
No	199 (89.2)	102 (89.5)	97 (89)	
Yes	24 (10.8)	12 (10.5)	12 (11)	
Pneumonia, n (%)				.33

XSL•FO
RenderX

Characteristics	Total (n=223)	No bone loss (n=114)	Bone loss (n=109)	*P* value
No	199 (89.2)	104 (91.2)	95 (87.2)	
Yes	24 (10.8)	10 (8.8)	14 (12.8)	
Infected segment, n (%)				.005
Cervical	14 (6.3)	13 (11.4)	1 (0.9)	
Thoracic	43 (19.3)	22 (19.3)	21 (19.3)	
Lumbar	157 (70.4)	75 (65.8)	82 (75.2)	
Thoracolumbar	9 (4.0)	4 (3.5)	5 (4.6)	
Number of infected vertebrae, n (%)				.97
1	10 (4.5)	5 (4.4)	5 (4.6)	
2	164 (73.5)	83 (72.8)	81 (74.3)	
≥3	49 (22.0)	26 (22.8)	23 (21.1)	
Localized kyphosis, n (%)				.62
No	177 (79.4)	92 (80.7)	85 (78)	
Yes	46 (20.6)	22 (19.3)	24 (22)	
Epidural abscess, n (%)				.20
No	170 (76.2)	91 (79.8)	79 (72.5)	
Yes	53 (23.8)	23 (20.2)	30 (27.5)	
Osteoporosis, n (%)				<.001
No	107 (48.0)	79 (69.3)	28 (25.7)	
Yes	116 (52.0)	35 (30.7)	81 (74.3)	
Laboratory parameters				
WBC[b], mean (SD)	7.5 (3.5)	7.4 (3.4)	7.6 (3.6)	.76
RBC[c], mean (SD)	4.0 (2.1)	3.9 (0.8)	4.2 (2.9)	.27
Hemoglobin, mean (SD)	112.5 (20.1)	111.0 (20.0)	114.1 (20.2)	.25
Platelet, mean (SD)	283.9 (117.3)	274.8 (111.3)	293.4 (123.1)	.24
CRP[d], median (IQR)	40.7 (14.0-84.0)	43.7 (16.2-90.6)	37.9 (11.0-73.1)	.16
ESR[e], mean (SD)	56.6 (33.2)	57.0 (35.2)	56.2 (31.1)	.87
Albumin, mean (SD)	35.3 (4.7)	37.3 (4.4)	33.2 (4.1)	<.001
IL-6[f], median (IQR)	26.7 (9.6-63.0)	21.5 (9.3-38.6)	33.1 (13.5-124.7)	.005
Activated partial thromboplastin time, mean (SD)	38.9 (6.5)	39.5 (6.3)	38.3 (6.7)	.17
Plasma fibrinogen, mean (SD)	5.1 (1.8)	3.9 (1.5)	6.4 (1.1)	<.001
Thrombin time, mean (SD)	18.8 (6.9)	19.4 (9.4)	18.2 (2.0)	.20
D-dimer, median (IQR)	0.9 (0.5-1.8)	1.0 (0.5-2.1)	0.9 (0.4-1.6)	.27

[a]MDRB: multidrug-resistant bacteria.
[b]WBC: white blood cell count.
[c]RBC: red blood cell.
[d]CRP: C-reactive protein.
[e]ESR: erythrocyte sedimentation rate.
[f]IL-6: interleukin-6.

Predictor Selection and Model Construction

Of the 31 baseline candidate predictors, 11 met the univariable screening criterion of $P \leq .20$ and were entered into LASSO regression. A penalty of $\lambda_1$se of 0.034 was selected using the 1 SE rule. At this penalty, 6 predictors retained nonzero coefficients: multidrug-resistant bacterial infection, infected spinal segment, osteoporosis, IL-6, albumin, and plasma

XSL•FO
RenderX

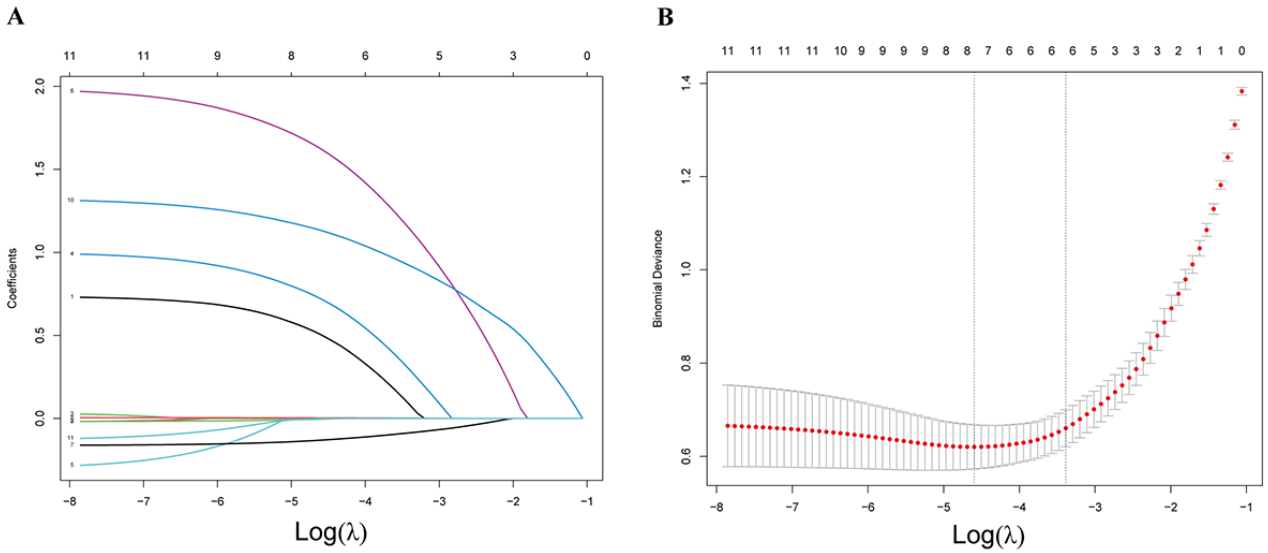
fibrinogen (Figure 2). These predictors were included together in the final multivariable logistic regression model. Infected spinal segment contributed 3 parameters. The model therefore included 8 predictor parameters, excluding the intercept. Regression coefficients, adjusted ORs, 95% CIs, and 2-sided *P* values are provided in Table 2.

Osteoporosis was associated with higher odds of postinfectious bone loss (adjusted OR 7.345, 95% CI 2.757-19.570; *P*<.001). Higher plasma fibrinogen was also associated with higher odds (adjusted OR 3.673 per 1 g/L increase, 95% CI 2.410-5.598; *P*<.001). Higher albumin was associated with lower odds (adjusted OR 0.834 per 1 g/L increase, 95% CI 0.749-0.929; *P*=.001). Cervical infection was the reference category. The adjusted OR was 14.041 for thoracic infection (95% CI 1.079-182.662; *P*=.04). The corresponding estimates were 28.876 for lumbar infection (95% CI 2.648-314.895; *P*=.006) and 12.604 for thoracolumbar infection (95% CI 0.436-364.075; *P*=.14). The adjusted OR for multidrug-resistant bacterial infection was 2.718 (95% CI 0.993-7.444; *P*=.05). For IL-6, the adjusted OR per 1 pg/mL increase was 1.004 (95% CI 0.996-1.012; *P*=.30).

As shown in Table S2 in Multimedia Appendix 1, the GVIFs for IL-6, plasma fibrinogen, and albumin ranged from 1.050 to 1.132, suggesting no substantial multicollinearity involving these continuous predictors. Restricted cubic spline analyses showed no statistically significant evidence of nonlinearity for IL-6 (*P*=.17), plasma fibrinogen (*P*=.18), or albumin (*P*=.68). The corresponding plots are provided in Figures S2-S4 in Multimedia Appendix 1.

The final model was presented as a nomogram to estimate the probability of postinfectious bone loss at 12 months (Figure 3). An illustrative patient case shows how to use the nomogram (Figure 4). The full regression coefficients, predictor coding, and prediction equation are provided in Table S3 in Multimedia Appendix 1.

Figure 2. Predictor selection using least absolute shrinkage and selection operator (LASSO) regression. (A) LASSO coefficient profiles showing changes in the coefficients of candidate predictors as the penalty parameter λ varied. (B) The penalty parameter λ was selected using 5-fold cross-validation and the 1 SE rule in the study cohort.



XSL•FO
RenderX

Table 2. Multivariable model for postinfectious bone loss (n=223).

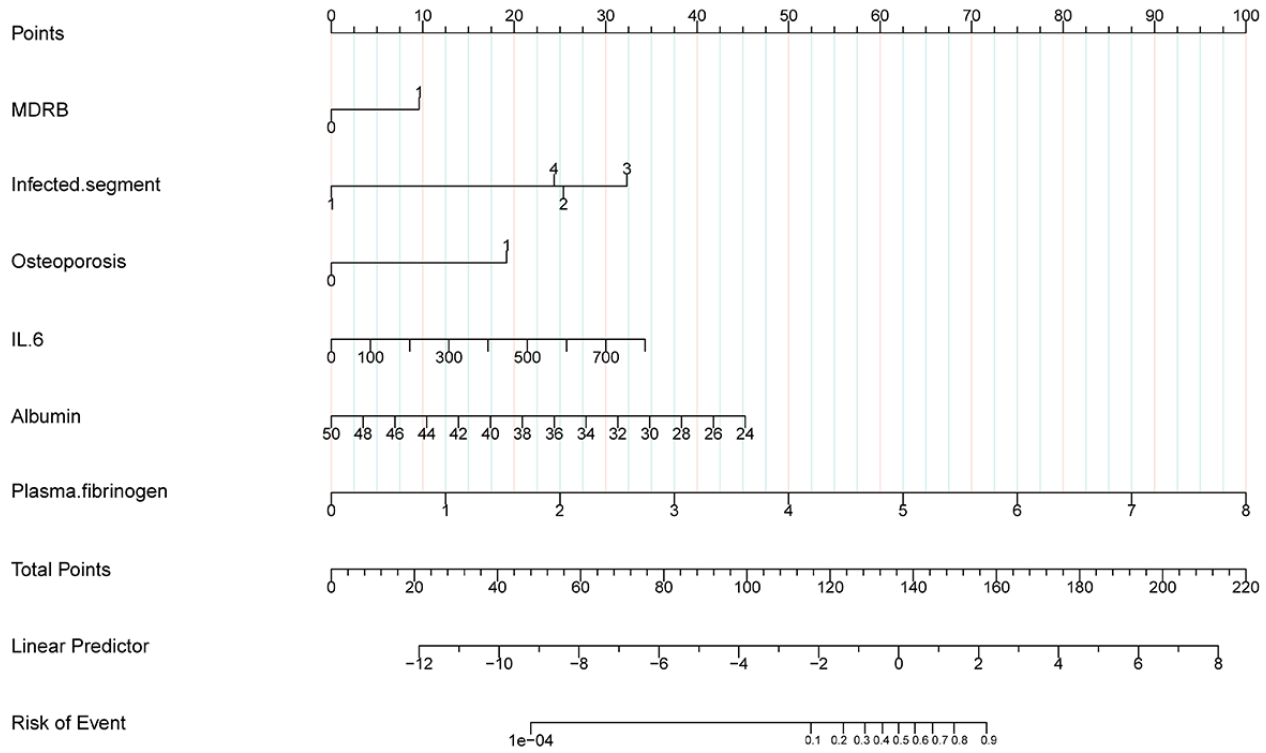
Predictor	β coefficient	SE	OR[a] (95% CI)	*P* value
Intercept	−5.144	2.426	—[b]	.03
Multidrug-resistant bacterial infection (yes vs no)	1.000	0.514	2.718 (0.993-7.444)	.05
Thoracic vs cervical infection	2.642	1.309	14.041 (1.079-182.662)	.04
Lumbar vs cervical infection	3.363	1.219	28.876 (2.648-314.895)	.006
Thoracolumbar vs cervical infection	2.534	1.716	12.604 (0.436-364.075)	.14
Osteoporosis (yes vs no)	1.994	0.500	7.345 (2.757-19.570)	<.001
IL-6[c], pg/mL	0.004	0.004	1.004 (0.996-1.012)	.30
Albumin, g/L	−0.181	0.055	0.834 (0.749-0.929)	.001
Plasma fibrinogen, g/L	1.301	0.215	3.673 (2.410-5.598)	<.001

[a]OR: odds ratio.

[b]Not applicable.

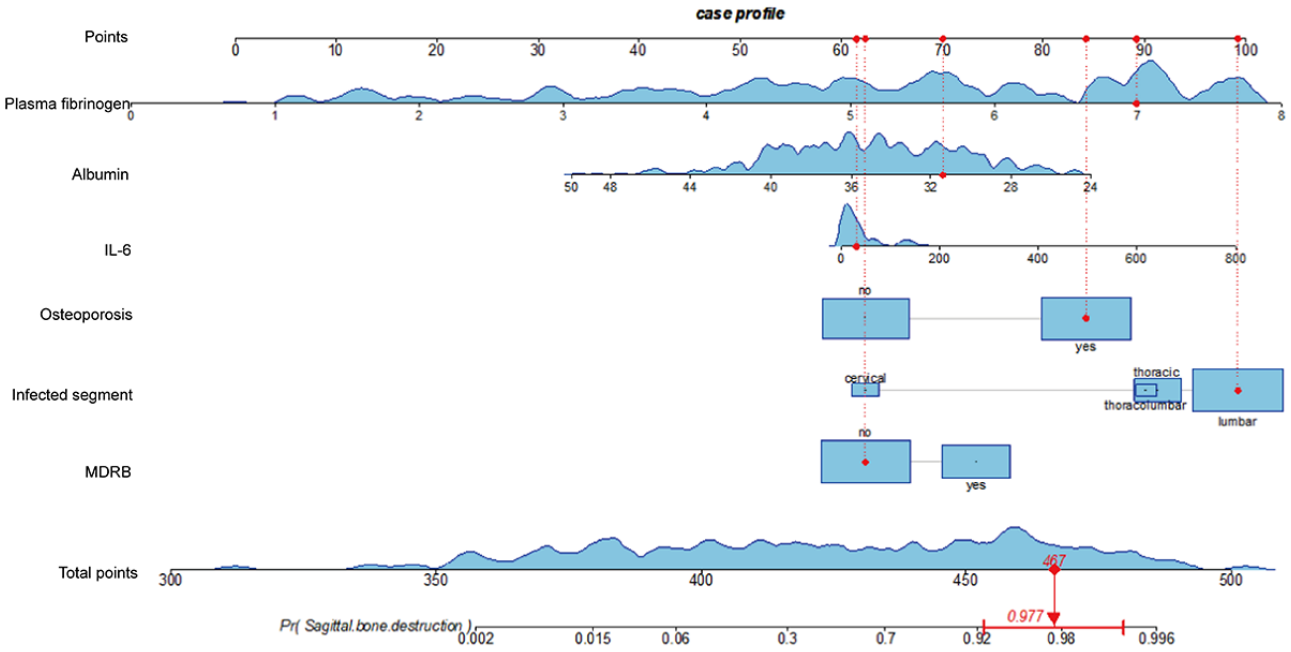
[c]IL-6: interleukin-6.

Figure 3. Nomogram for predicting the risk of postinfectious bone loss in patients with spinal infection. To use the nomogram, add up the points assigned to each predictor to calculate the total score. Then, draw a vertical line from the corresponding position on the total points axis to the risk of event scale to determine the predicted probability (MDRB and osteoporosis: 0=absent and 1=present; infected spinal segment: 1=cervical, 2=thoracic, 3=lumbar, and 4=thoracolumbar). IL-6: interleukin-6; MDRB: multidrug-resistant bacteria.



XSL•FO
RenderX

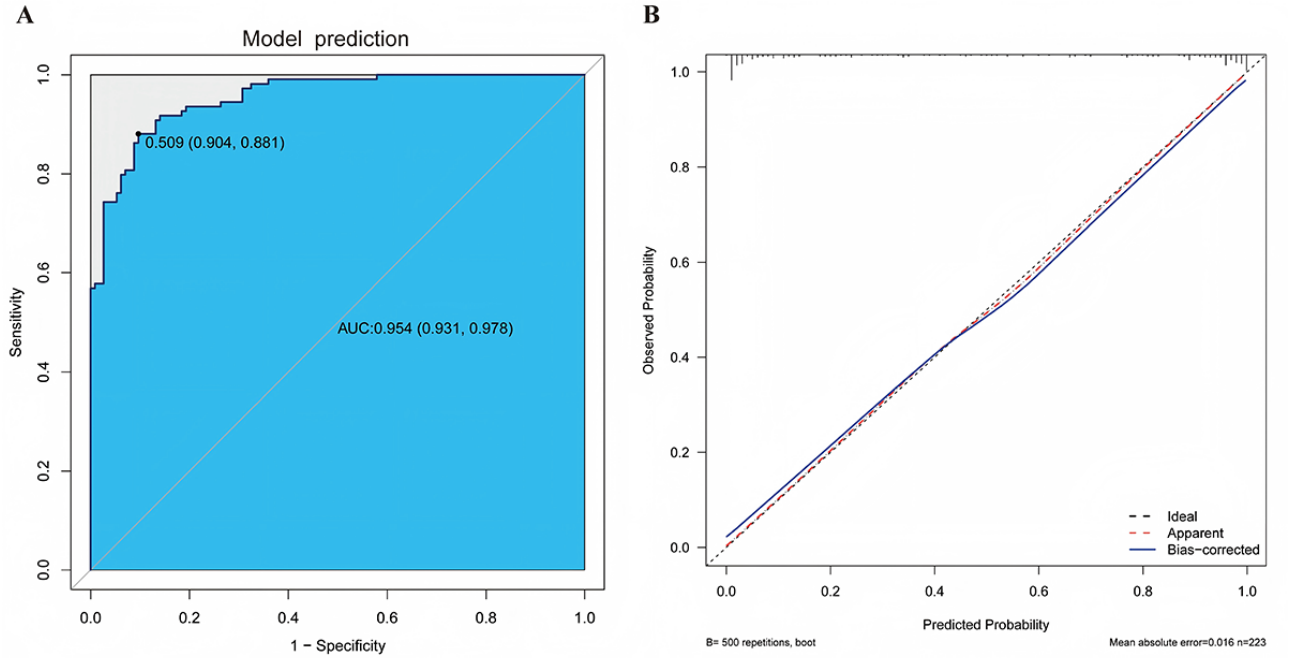
Figure 4. Illustrative patient case demonstrating the use of the nomogram to predict postinfectious bone loss. A patient with lumbar spinal infection and osteoporosis, without multidrug-resistant bacterial infection (MDRB), had baseline plasma fibrinogen, albumin, and interleukin-6 (IL-6) concentrations of 6.99 g/L, 31.4 g/L, and 30.82 pg/mL, respectively. Red dots and dotted lines indicate the patient's predictor values and corresponding points. The 6 scores summed to approximately 467 points, corresponding to a predicted probability of 0.977 (97.7%) for postinfectious bone loss at 12 months. The patient subsequently developed postinfectious bone loss, as assessed by computed tomography (CT) at 12 months.



Model Performance and Internal Validation

The model achieved an apparent AUC of 0.954 (95% CI 0.931-0.978; Figure 5A). Internal validation using 500 bootstrap resamples yielded an optimism-corrected AUC of 0.946 (95% CI 0.919-0.972), with a sensitivity of 86.2% and a specificity of 88.6%, as shown in Figure S5 in Multimedia Appendix 1. Calibration curves showed agreement between predicted and observed risks, with a mean absolute error of 0.016 (Figure 5B). The calibration intercept was 0.00 (95% CI −0.43 to 0.43), and the calibration slope was 1.00 (95% CI 0.75-1.25). The Brier score was 0.096 (95% CI 0.064-0.118).

Figure 5. Receiver operating characteristic (ROC) and calibration curves of the nomogram for predicting postinfectious bone loss. (A) ROC curve in the study cohort. (B) Calibration curves before and after optimism correction using 500 bootstrap resamples. AUC: area under the receiver operating characteristic curve.

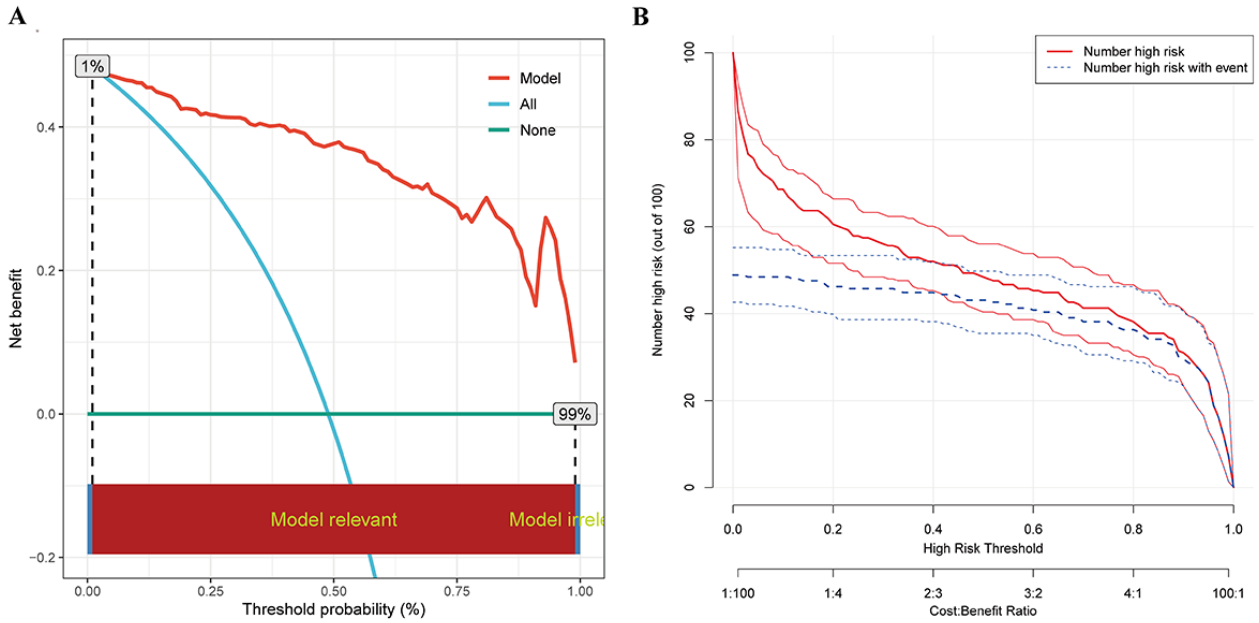


XSL•FO
RenderX

Potential Clinical Utility

DCA showed higher estimated net benefit for the nomogram than for the "treat-all" and "treat-none" strategies over a range of threshold probabilities (Figure 6A). The CIC showed the numbers of high-risk patients and true-positive cases per 100 patients (Figure 6B). As the threshold increased, fewer patients were classified as high risk, and the gap between these counts narrowed. These exploratory findings suggest potential value for risk stratification within this cohort.

Figure 6. Decision curve analysis (DCA) and clinical impact curve of the nomogram for predicting postinfectious bone loss in the study cohort. (A) DCA of the nomogram. (B) Clinical impact curve of the nomogram.



Discussion

Support for the Original Hypotheses

This study developed and internally validated a nomogram to predict the risk of postinfectious bone loss at 12 months in patients with spinal infection. The model included 6 baseline predictors: multidrug-resistant bacterial infection, infected spinal segment, osteoporosis, IL-6, albumin, and plasma fibrinogen. The apparent AUC was 0.954 (95% CI 0.931-0.978; Figure 5A). Internal validation using 500 bootstrap resamples yielded an optimism-corrected AUC of 0.946 (95% CI 0.919-0.972).

Calibration plots showed good agreement between predicted probabilities and observed outcomes. Exploratory DCA suggested potential net benefit, while the CIC illustrated the numbers of patients classified as high risk and true-positive cases across risk thresholds. These findings provide preliminary support for the potential value of the nomogram in early risk stratification within this cohort.

Similarity of Results

An increased risk of postinfectious bone loss is associated with multiple factors.

Albumin was included as a baseline predictor in our model, with lower levels potentially associated with greater odds of postinfectious bone loss. The direction of this association was consistent with previous observational studies linking hypoalbuminemia to osteoporosis in other populations [37,38]. Notably, Zhao et al [10] also included lower albumin levels in their nomogram for predicting postoperative bone nonunion in patients with infectious spondylitis. Nagayama et al [39] found that lower serum albumin levels were independently associated with osteoporosis in postmenopausal patients with rheumatoid arthritis. Furthermore, Kunutsor et al [40] found that lower baseline serum albumin levels were associated with an increased risk of a composite outcome of hip, humeral, or wrist fractures, and this association persisted after adjustment for multiple confounders. These findings suggest a possible association between lower albumin levels and adverse skeletal outcomes, providing indirect support for our findings.

In addition to these laboratory markers, osteoporosis was another predictor in the present model. However, our findings regarding osteoporosis differed from those of a previous study: osteoporosis was associated with greater odds of postinfectious bone loss in our model. By contrast, Hockmann et al [7] reported no statistically significant difference in osteoporosis between severe and mild-to-moderate destruction groups. Their finding came from an unadjusted comparison, and few patients had documented osteoporosis. These features may have limited the ability to detect a difference. Their study also classified existing destruction, whereas the present study assessed a defined CT outcome at 12 months. Differences in osteoporosis assessment, statistical adjustment, and outcome timing may partly explain the different findings.

Furthermore, previous studies have found that infection with antibiotic-resistant bacteria is associated with adverse clinical

XSL•FO
RenderX

outcomes in patients with spinal infection. Saad Berreta et al [41] reported more frequent surgery, postoperative complications, and reoperation in patients with methicillin-resistant *Staphylococcus aureus* (MRSA) spinal infection than in those with methicillin-susceptible *S aureus* spinal infection. Nishizawa et al [42] also found that MRSA infection was associated with postoperative recurrence. These findings are consistent with ours in linking antibiotic-resistant bacterial infection to poorer outcomes. However, differences in the types of resistant bacteria and study outcomes mean that they provide only indirect support for the association with postinfectious bone loss.

Additionally, in developing their models, both Li et al [9] and Zhao et al [10] performed initial univariable screening, followed by LASSO for further predictor selection, and then fitted multivariable logistic regression models. Zhang et al [28,29] also performed univariable screening before LASSO, consistent with the analytical approach used in our study. Both spinal infection studies used the entire cohort for model development, an approach we also adopted to make efficient use of limited clinical data.

Interpretation

Regarding model development and internal validation, our analytical strategy was guided by the number of candidate predictors and the size of the available cohort. Among the 436 patients assessed for eligibility, 223 fulfilled the inclusion criteria and formed the model development cohort. We considered 31 candidate predictors spanning baseline clinical characteristics, laboratory parameters, and imaging measurements to assess information relevant to predicting postinfectious bone loss across multiple domains. Given the large number of candidate predictors and the relatively limited sample size, we combined univariable screening with LASSO to reduce the number of variables entering the multivariable model while retaining potentially informative predictors and controlling model complexity. To complement this approach, bootstrap resampling was used for internal validation to make efficient use of the available data and assess the predictive performance of the entire model development procedure. This approach allows the full cohort to contribute to final model development while avoiding the loss of precision and increased variability in performance estimates associated with a single random data split [43]. Although leave-one-out cross-validation also uses the available data efficiently, changes in the training-sample event proportion when a patient with or without an event is omitted can bias the pooled AUC estimate downward [44]. Bootstrap validation, with the entire model development process repeated within each resample, was therefore adopted to assess discrimination and calibration while accounting for optimism arising from predictor selection and model fitting [34].

In terms of the clinical interpretation of the selected predictors, osteoporosis, lower albumin levels, and higher fibrinogen levels were associated with postinfectious bone loss at 12 months, suggesting that subsequent vertebral destruction may reflect both the infection itself and underlying skeletal health and systemic illness. Although all patients had a vertebral destruction ratio below one-third at diagnosis, nearly half met the predefined outcome at follow-up. This finding indicates that patients with limited initial structural damage remain at risk of further bone destruction and warrant attention during follow-up.

To interpret the association with underlying skeletal health, it is first necessary to distinguish baseline osteoporosis from the subsequent structural outcome. Osteoporosis was defined according to the 2023 Official Positions of the International Society for Clinical Densitometry (ISCD). In postmenopausal women and men aged 50 years or older, a T-score of less than or equal to −2.5 at the lumbar spine, total hip, or femoral neck met the bone density criterion for osteoporosis [19]. Osteoporosis was entered into the model as a binary variable. As a baseline predictor, osteoporosis was assessed during the initial diagnostic evaluation, when other candidate predictors were collected and baseline CT confirmed that all included patients had a vertebral bone destruction ratio below one-third. Postinfectious bone loss was defined as a vertebral bone destruction ratio of at least one-third on CT at 12 months after baseline. The CT-based vertebral bone destruction height ratio provides a quantitative basis for outcome classification. The observed interobserver agreement supports the reproducibility of this classification. Collectively, baseline osteoporosis and postinfectious bone loss at follow-up were assessed at different time points using distinct criteria based on bone density and local vertebral structural destruction, respectively, avoiding direct circularity between the predictor and outcome definitions.

Furthermore, with this distinction established, the association between osteoporosis and subsequent local bone destruction suggests that underlying skeletal fragility may influence structural damage and repair following infection. In a rat model of fracture-related infection, Li et al [45] found that osteoporotic animals had a higher bacterial burden at the infection site, more extensive osteolysis, and delayed healing. These findings provide experimental support for our observations but do not establish that the same mechanisms operate in infected human vertebrae.

In addition to baseline skeletal fragility, the selected laboratory predictors provide a complementary perspective on the systemic condition of patients at diagnosis. The associations of albumin and fibrinogen with the outcome suggest that systemic illness at diagnosis may provide prognostic information about subsequent bone destruction. Albumin levels are influenced by inflammation and changes in protein synthesis and distribution. Lower albumin levels therefore cannot be attributed solely to malnutrition and may also reflect infection-related inflammatory activity and overall illness burden [46,47]. Fibrinogen participates in coagulation and the acute-phase response, and elevated levels may reflect the inflammatory and coagulation changes accompanying infection [48]. Our findings therefore suggest that risk assessment for bone loss in patients with spinal infection should consider the patients' systemic condition alongside local disease features.

Within this broader clinical context, pathogen resistance and the host inflammatory response offer further information relevant to infection-related outcomes. Multidrug-resistant bacterial infection and IL-6 reflect pathogen resistance and the

XSL•FO
RenderX

host inflammatory response, respectively. Previous research has linked MRSA spinal infection to postoperative recurrence [42], suggesting that antimicrobial resistance may make infection control more challenging. Regarding IL-6, Brinkmann et al [49] found significantly higher preoperative serum levels in patients with vertebral osteomyelitis than in those with degenerative spinal disease in a prospective clinical study, supporting its interpretation as a marker of infection-related inflammation. In this study, resistance status and IL-6 were incorporated into the model alongside skeletal status, infected spinal segment, and other laboratory parameters to estimate the risk of postinfectious bone loss at 12 months.

Alongside these patient-level and infection-related characteristics, the model also incorporated the anatomical location of the infection. Infected spinal segment reflects the anatomical location of the lesion. In this study, it was classified as cervical, thoracic, lumbar, or thoracolumbar and entered as a nominal categorical variable using dummy coding, with cervical infection as the reference category. This approach avoided imposing ordinal or linear assumptions on the anatomical categories. However, the small sample sizes and limited numbers of events in the cervical and thoracolumbar groups may have reduced the precision of the adjusted OR estimates, resulting in wide CIs. Therefore, comparisons of the associations between infected segments and bone loss should not rely solely on adjusted OR point estimates but should also consider the corresponding 95% CIs, the patient's overall clinical condition, and other relevant predictors.

Beyond individual associations, the overall performance of the model helps assess its value for prediction. Strong discrimination indicates separation between patients with and without the later outcome. Calibration assesses agreement between predicted probabilities and observed outcomes, while the Brier score summarizes error in the predicted probabilities. Considering these measures together provides a broader assessment than discrimination alone [33]. The modest reduction in AUC after optimism correction is consistent with limited estimated optimism in discrimination. Repeating the complete development procedure during bootstrap validation allowed that estimate to reflect variable selection and coefficient fitting [43]. These findings inform the interpretation of the complete prediction procedure within this cohort.

Furthermore, to assess potential overfitting, we performed internal validation using 500 bootstrap resamples with optimism correction. The optimism-corrected AUC indicated that the model retained good discrimination after correction within this cohort. Beyond discrimination, exploratory DCA and CIC analyses suggested potential net benefit across the evaluated risk thresholds and illustrated the corresponding numbers of patients classified as high risk and those who subsequently developed bone loss. These findings suggest that the nomogram may support individualized risk assessment and inform clinical reassessment and imaging follow-up decisions. However, internal validation and exploratory utility analyses do not establish effectiveness in clinical practice. Independent external validation and prospective clinical impact studies are needed to assess generalizability and determine whether model-informed assessment improves clinical decisions and patient outcomes.

Limitations

This study has several limitations. First, the single-center retrospective design relied on existing medical records, and the requirements for pathogen identification results, complete key clinical data, and follow-up CT imaging restricted inclusion to patients with complete data. If patients with missing data differed systematically from those included, this restriction may have introduced selection bias and limited the representativeness of the study population [50]. We used consecutive sampling and checked data completeness, logical consistency, coding, and measurement units, correcting identified errors against the original records to reduce errors in data extraction and recording. However, these measures could not eliminate selection bias arising from the eligibility criteria. Future multicenter prospective studies should include broader patient populations to assess the applicability of the findings.

Second, the relatively limited sample size and large number of initial candidate predictors may have increased the risk of overfitting and instability in predictor selection [51]. Univariable screening before LASSO may also have excluded variables with potential predictive value [34]. To control model complexity, we used LASSO with the 1 SE rule for predictor selection and developed the model using the entire cohort. We then repeated the complete modeling procedure in 500 bootstrap resamples to estimate and correct optimism in model performance [34]. These measures reduced information loss from data splitting and allowed assessment of optimism arising from model development, but could not fully exclude overfitting [52]. Further research in larger cohorts should examine the consistency of predictor selection and evaluate the relative predictive performance of different modeling approaches.

Third, small sample sizes and limited outcome events in some infected-segment categories may have resulted in unstable effect estimates and wide CIs [53]. We treated infected spinal segment as a nominal categorical variable using dummy coding to avoid unjustified ordinal or linear assumptions, and reported adjusted ORs with 95% CIs to convey estimation uncertainty. However, appropriate coding could not compensate for sparse data. Larger cohorts with greater representation of each anatomical category are needed to better characterize these associations.

Fourth, the model used information available at initial diagnosis and did not account for changes in infection status or treatment response during follow-up. To maintain a consistent prediction time point, we used baseline predictors and defined the target as the CT outcome at 12 months, making the model applicable to risk assessment at diagnosis. Nevertheless, baseline predictions may not fully capture subsequent changes in risk as the disease and treatment course evolve. Future studies could incorporate repeated clinical and laboratory measurements to develop dynamic risk prediction models [54]. In addition, although the one-third threshold provides a criterion for outcome classification, the binary outcome cannot fully capture the continuous variation in the extent of vertebral bone destruction. Future studies should therefore incorporate more precise continuous quantitative measures and advanced imaging assessment methods.

XSL•FO
RenderX

Finally, independent external validation and prospective clinical impact evaluation have not yet been performed, leaving the model's generalizability and clinical utility uncertain [52]. We assessed model performance through bootstrap internal validation and examined discrimination, calibration, the Brier score, and exploratory DCA and CIC to evaluate its predictive performance and potential applications. However, these analyses cannot replace external validation or demonstrate that model-guided follow-up improves patient outcomes [52,55,56]. Future studies should validate the model in independent multicenter cohorts and prospectively evaluate its effects on follow-up decisions, resource use, and patient outcomes.

Generalizability

The findings are most relevant to patients with pathogen-confirmed spinal infections and a vertebral destruction ratio less than one-third at diagnosis who receive care in settings similar to the study center. Although the cohort included different pathogen types, infected spinal segments, and osteoporosis statuses, this diversity was confined to patients meeting the eligibility criteria at a single specialist center. Applicability to other populations may depend on differences in patient characteristics, pathogen distributions, and measurement methods [52]. Multicenter external validation in relevant target populations is therefore needed to assess discrimination, calibration, and clinical utility before broader use of the model for predicting postinfectious bone loss [35].

Implications

The nomogram may provide additional information when considering whether patients at higher estimated risk of postinfectious bone loss warrant closer reassessment. In practice, the estimated risk would need to be considered alongside the patient's current clinical status, with decisions about additional imaging also taking account of symptoms, neurological findings, and changes in laboratory parameters [57]. Beyond individual assessment, risk estimates may support discussions with patients about follow-up priorities and the purpose of planned examinations. Furthermore, to explore these potential applications in routine practice, an online calculator could be considered following external validation, drawing on published examples of online prediction applications [58]. Such a format may make individual risk estimates easier to obtain and discuss during consultations.

Conclusions

This study developed a visual nomogram integrating baseline clinical characteristics, imaging features, and laboratory parameters for individualized prediction of 12-month postinfectious bone loss in patients with spinal infection. By combining complementary clinical information into a single risk estimate, this study extends previous association studies and provides a practical framework for assessing subsequent bone loss risk. The model showed good discrimination and calibration in internal validation. Its potential clinical contribution lies in identifying patients who may warrant closer monitoring and timely reassessment before further structural deterioration. The resulting risk estimates may support more individualized follow-up planning alongside the patient's clinical status.

Acknowledgments

The authors sincerely thank all the individuals and institutions that have contributed to this research.

Funding

This study was supported by the National Natural Science Foundation of China (grant number 82202701), the Natural Science Foundation of Shandong Province (grant number ZR2022QH184), the Taishan Scholars Program, and the Shandong Provincial Medical Association. All funding was awarded to CZ.

Data Availability

The data supporting the findings of this study are available from the corresponding author upon reasonable request.

Generative AI Use

Generative AI tools (GPT-6, OpenAI) were used solely to assist in identifying potentially relevant literature and improving the English language of the manuscript, including grammar, clarity, and readability. AI tools were not used for study design, data collection or analysis, or the formulation of scientific conclusions. All content was reviewed and verified by the authors, who take full responsibility for the final manuscript.

Authors' Contributions

Conceptualization: CZ
Formal analysis: XC, SK, RD, CZ
Investigation: XC, SK, CZ, GW, YL, FZ
Resources: CZ, SK, RD, GW, HT, JS, FZ
Visualization: XC, SK, RD, CZ
Writing – original draft: XC, SK, CZ

XSL•FO
RenderX

Conflicts of Interest

None declared.

Multimedia Appendix 1

Supplementary figures and tables for the prediction of postinfectious bone loss after spinal infection.
[DOCX File , 380 KB-Multimedia Appendix 1]

References

1. Phan VT, Dimou J, Davidson AS, Giulieri S, Silver J, Yoon SW, et al. Spinal infection: an evolving clinical and public health challenge. J Clin Neurosci. 2026;147:111949. [doi: 10.1016/j.jocn.2026.111949] [Medline: 41740215]
2. Sheidae Mehne Z, Honarjou E, Khamoushi Kahdouee M. Chronic infections of the spine: a systematic review of microbial etiologies, diagnostic approaches, and treatment outcomes. Int J Infect Dis. 2026;169:108769. [FREE Full text] [doi: 10.1016/j.ijid.2026.108769] [Medline: 42140478]
3. Kramer A, Thavarajasingam SG, Neuhoff J, Davies B, Barbagallo G, Debono B, et al. Diagnosis and management of de novo non-specific spinal infections: European Association of Neurosurgical Societies (EANS) Spine Section Delphi consensus recommendations. Brain Spine. 2025;5:104178. [FREE Full text] [doi: 10.1016/j.bas.2024.104178] [Medline: 39866360]
4. Campbell MJ, Bustamante-Gomez C, Fu Q, Beenken KE, Reyes-Pardo H, Smeltzer MS, et al. RANKL-mediated osteoclast formation is required for bone loss in a murine model of Staphylococcus aureus osteomyelitis. Bone. 2024;187:117181. [FREE Full text] [doi: 10.1016/j.bone.2024.117181] [Medline: 38960295]
5. Cao H, Xue F. Spinal infections. Front Neurosci. 2026;20:1864932. [FREE Full text] [doi: 10.3389/fnins.2026.1864932] [Medline: 42422255]
6. Kramer A, Neuhoff J, Thavarajasingam SG, Sutherland R, McCaughan H, Davies B, et al. Evaluation of spinal deformity and its progression in pyogenic spondylodiscitis: a retrospective MRI study of 59 cases. Brain Spine. 2025;5:104204. [FREE Full text] [doi: 10.1016/j.bas.2025.104204] [Medline: 40007800]
7. Hockmann JP, Kernich N, Sircar K, Eysel P, Hoffmann A, Jochimsen D, et al. Severe destruction in vertebral osteomyelitis - risk factors and survival. Infection. 2026;54(2):741-747. [doi: 10.1007/s15010-025-02701-x] [Medline: 41284212]
8. Lang S, Bachtler M, Straub J, Krückel J, Baertl S, Ardelt M, et al. Segmentation-based 3D volumetry and linear regression modeling for assessing the vertebral bone loss in pyogenic vertebral osteomyelitis. Eur Spine J. 2025;34(10):4705-4716. [doi: 10.1007/s00586-025-09163-7] [Medline: 40715674]
9. Li J, Zhao Y, Xu L, Yang Y, Ruan W, Dang R, et al. Nomogram for predicting inadequate treatment response in vertebral osteomyelitis. Ann Med. 2026;58(1):2648906. [FREE Full text] [doi: 10.1080/07853890.2026.2648906] [Medline: 41918281]
10. Zhao W, Xing L, Yang Y, Ruan W, Li J, Dang R, et al. Development and internal validation of a nomogram for predicting postoperative bone nonunion in infectious spondylitis: a retrospective cohort study. Ann Med. 2026;58(1):2709091. [doi: 10.1080/07853890.2026.2709091] [Medline: 42517740]
11. Li J, Zhao Y, Yang Y, Ruan W, Dang R, Zhao W, et al. Development and validation of a nomogram for predicting mortality in patients with vertebral osteomyelitis. Infection. 2026;54(2):971-981. [doi: 10.1007/s15010-026-02741-x] [Medline: 41758454]
12. Schömig F, Taheri N, El-Sharkawi M, Aly MM, Yurac R, Camino Willhuber G, et al. The modified spinal instability spondylodiscitis score (mSISS): adaptation and validation of a novel classification system for spinal instability in spondylodiscitis. Global Spine J. 2026:21925682261455309. [FREE Full text] [doi: 10.1177/21925682261455309] [Medline: 42189054]
13. Iasonos A, Schrag D, Raj GV, Panageas KS. How to build and interpret a nomogram for cancer prognosis. J Clin Oncol. 2008;26(8):1364-1370. [doi: 10.1200/JCO.2007.12.9791] [Medline: 18323559]
14. Wang J, Li Z, Chi X, Chen Y, Wang H, Wang X, et al. Development of a diagnostic model for differentiating tuberculous spondylitis and pyogenic spondylitis with MRI: a multicenter retrospective observational study. Spine (Phila Pa 1976). 2024;49(1):34-45. [FREE Full text] [doi: 10.1097/BRS.0000000000004848] [Medline: 37796171]
15. Riley RD, Snell KI, Ensor J, Burke DL, Harrell FE, Moons KG, et al. Minimum sample size for developing a multivariable prediction model: PART II - binary and time-to-event outcomes. Stat Med. 2019;38(7):1276-1296. [FREE Full text] [doi: 10.1002/sim.7992] [Medline: 30357870]
16. Sato T, Yamada K, Yasui K, Okumura J, Kanayama M, Hyakkan R, et al. Risk factors for delayed diagnosis of pyogenic spondylitis: a cross-sectional study with prospective case series. Spine Surg Relat Res. 2025;9(4):485-491. [doi: 10.22603/ssrr.2024-0320] [Medline: 40786933]
17. Foreman SC, Schwaiger BJ, Gempt J, Jungmann PM, Kehl V, Delbridge C, et al. MR and CT imaging to optimize CT-guided biopsies in suspected spondylodiscitis. World Neurosurg. 2017;99:726-734.e7. [doi: 10.1016/j.wneu.2016.11.017] [Medline: 27840205]

XSL•FO
RenderX

18. Lener S, Hartmann S, Barbagallo GMV, Certo F, Thomé C, Tschugg A. Management of spinal infection: a review of the literature. Acta Neurochir (Wien). 2018;160(3):487-496. [FREE Full text] [doi: 10.1007/s00701-018-3467-2] [Medline: 29356895]
19. Slart RHJA, Punda M, Ali DS, Bazzocchi A, Bock O, Camacho P, et al. Updated practice guideline for dual-energy X-ray absorptiometry (DXA). Eur J Nucl Med Mol Imaging. 2025;52(2):539-563. [FREE Full text] [doi: 10.1007/s00259-024-06912-6] [Medline: 39316095]
20. Magiorakos A, Srinivasan A, Carey RB, Carmeli Y, Falagas ME, Giske CG, et al. Multidrug-resistant, extensively drug-resistant and pandrug-resistant bacteria: an international expert proposal for interim standard definitions for acquired resistance. Clin Microbiol Infect. 2012;18(3):268-281. [FREE Full text] [doi: 10.1111/j.1469-0691.2011.03570.x] [Medline: 21793988]
21. Gou L, Yang Y, Li J, Cai L, Xing W, Liu W, et al. MRI findings and classification of brucella spondylitis: a China multicenter study. Eur J Med Res. 2024;29(1):469. [FREE Full text] [doi: 10.1186/s40001-024-02011-2] [Medline: 39342400]
22. Golimbu C, Firooznia H, Rafii M. CT of osteomyelitis of the spine. AJR Am J Roentgenol. 1984;142(1):159-163. [doi: 10.2214/ajr.142.1.159] [Medline: 6606951]
23. Huang C, Chen X, Kuang S, Dang R, Li Y, Wang G, et al. Risk factors and a diagnostic nomogram for early prediction of gram-positive coccal etiology in spontaneous spinal infection. Infection. 2026;54(4):2019-2031. [doi: 10.1007/s15010-026-02831-w] [Medline: 42201512]
24. Miskin N, Gaviola GC, Huang RY, Kim CJ, Lee TC, Small KM, et al. Intra- and intersubspecialty variability in lumbar spine MRI interpretation: a multireader study comparing musculoskeletal radiologists and neuroradiologists. Curr Probl Diagn Radiol. 2020;49(3):182-187. [doi: 10.1067/j.cpradiol.2019.05.003] [Medline: 31133459]
25. Vanbelle S, Engelhart C, Blix E. A comprehensive guide to study the agreement and reliability of multi-observer ordinal data. BMC Med Res Methodol. 2024;24(1):310. [FREE Full text] [doi: 10.1186/s12874-024-02431-y] [Medline: 39707223]
26. Landis JR, Koch GG. The measurement of observer agreement for categorical data. Biometrics. 1977;33(1):159-174. [Medline: 843571]
27. Collins GS, Reitsma JB, Altman DG, Moons KGM. Transparent reporting of a multivariable prediction model for individual prognosis or diagnosis (TRIPOD): the TRIPOD statement. BMJ. 2015;350:g7594. [FREE Full text] [doi: 10.1136/bmj.g7594] [Medline: 25569120]
28. Zhang G, Wang D, Chen F, Liu Y, Wang L, Jiao Y. Risk factors analysis and prediction model for malignant cerebral edema following mechanical thrombectomy in patients with large vessel occlusive stroke. Clin Appl Thromb Hemost. 2026;32:10760296261458526. [FREE Full text] [doi: 10.1177/10760296261458526] [Medline: 42240031]
29. Zhang J, Li H, Fang G, Zhu Z, Li X, Chen Y, et al. Development of a LASSO dynamic prediction system for interbody cage subsidence following OLIF surgery. NPJ Digit Med. 2025;8(1):656. [FREE Full text] [doi: 10.1038/s41746-025-02019-w] [Medline: 41233509]
30. Friedman J, Hastie T, Tibshirani R. Regularization paths for generalized linear models via coordinate descent. J Stat Softw. 2010;33(1):1-22. [FREE Full text] [Medline: 20808728]
31. Harris JK. Primer on binary logistic regression. Fam Med Community Health. 2021;9(Suppl 1):e001290. [FREE Full text] [doi: 10.1136/fmch-2021-001290] [Medline: 34952854]
32. Discacciati A, Palazzolo MG, Park J, Melloni GEM, Murphy SA, Bellavia A. Estimating and presenting non-linear associations with restricted cubic splines. Int J Epidemiol. 2025;54(4):dyaf088. [FREE Full text] [doi: 10.1093/ije/dyaf088] [Medline: 40527479]
33. Steyerberg EW, Vickers AJ, Cook NR, Gerds T, Gonen M, Obuchowski N, et al. Assessing the performance of prediction models: a framework for traditional and novel measures. Epidemiology. 2010;21(1):128-138. [FREE Full text] [doi: 10.1097/EDE.0b013e3181c30fb2] [Medline: 20010215]
34. Efthimiou O, Seo M, Chalkou K, Debray T, Egger M, Salanti G. Developing clinical prediction models: a step-by-step guide. BMJ. 2024;386:e078276. [FREE Full text] [doi: 10.1136/bmj-2023-078276] [Medline: 39227063]
35. Riley RD, Archer L, Snell KIE, Ensor J, Dhiman P, Martin GP, et al. Evaluation of clinical prediction models (part 2): how to undertake an external validation study. BMJ. 2024;384:e074820. [FREE Full text] [doi: 10.1136/bmj-2023-074820] [Medline: 38224968]
36. Kerr KF, Brown MD, Zhu K, Janes H. Assessing the clinical impact of risk prediction models with decision curves: guidance for correct interpretation and appropriate use. J Clin Oncol. 2016;34(21):2534-2540. [FREE Full text] [doi: 10.1200/JCO.2015.65.5654] [Medline: 27247223]
37. Afshinnia F, Wong KK, Sundaram B, Ackermann RJ, Pennathur S. Hypoalbuminemia and osteoporosis: reappraisal of a controversy. J Clin Endocrinol Metab. 2016;101(1):167-175. [FREE Full text] [doi: 10.1210/jc.2015-3212] [Medline: 26600169]
38. Afshinnia F, Pennathur S. Association of hypoalbuminemia with osteoporosis: analysis of the national health and nutrition examination survey. J Clin Endocrinol Metab. 2016;101(6):2468-2474. [FREE Full text] [doi: 10.1210/jc.2016-1099] [Medline: 27144935]

XSL•FO
RenderX

39. Nagayama Y, Ebina K, Tsuboi H, Hirao M, Hashimoto J, Yoshikawa H, et al. Low serum albumin concentration is associated with increased risk of osteoporosis in postmenopausal patients with rheumatoid arthritis. J Orthop Sci. 2022;27(6):1283-1290. [doi: 10.1016/j.jos.2021.08.018] [Medline: 34696921]
40. Kunutsor SK, Voutilainen A, Whitehouse MR, Seidu S, Kauhanen J, Blom AW, et al. Serum albumin and future risk of hip, humeral, and wrist fractures in Caucasian men: new findings from a prospective cohort study. Med Princ Pract. 2019;28(5):401-409. [FREE Full text] [doi: 10.1159/000499738] [Medline: 30893707]
41. Saad Berreta R, Zhang H, Alsoof D, McDonald CL, Diebo BG, Kuris E, et al. Beta-lactam-resistant Staphylococcus aureus in spinal osteomyelitis and spondylodiscitis: current landscape in antibiotic resistance, treatment, and complications. J Neurosurg Spine. 2023:1-6. [doi: 10.3171/2023.2.SPINE221353] [Medline: 36933262]
42. Nishizawa M, Djurasovic M, Glassman SD, Crawford CH, Dimar JR, Owens RK, et al. Clinical characteristics and surgical outcomes of spinal infection caused by methicillin-resistant Staphylococcus aureus. Spine J. 2026;26(2):272-279. [doi: 10.1016/j.spinee.2025.07.029] [Medline: 40653018]
43. Steyerberg EW, Harrell FE, Borsboom GJ, Eijkemans MJ, Vergouwe Y, Habbema JD. Internal validation of predictive models: efficiency of some procedures for logistic regression analysis. J Clin Epidemiol. 2001;54(8):774-781. [doi: 10.1016/s0895-4356(01)00341-9] [Medline: 11470385]
44. Geroldinger A, Lusa L, Nold M, Heinze G. Leave-one-out cross-validation, penalization, and differential bias of some prediction model performance measures-a simulation study. Diagn Progn Res. 2023;7(1):9. [FREE Full text] [doi: 10.1186/s41512-023-00146-0] [Medline: 37127679]
45. Li J, Wong RMY, Chung YL, Leung SSY, Chow SK, Ip M, et al. Fracture-related infection in osteoporotic bone causes more severe infection and further delays healing. Bone Joint Res. 2022;11(2):49-60. [FREE Full text] [doi: 10.1302/2046-3758.112.BJR-2021-0299.R1] [Medline: 35100815]
46. Evans DC, Corkins MR, Malone A, Miller S, Mogensen KM, Guenter P, et al. ASPEN Malnutrition Committee. The use of visceral proteins as nutrition markers: an ASPEN position paper. Nutr Clin Pract. 2021;36(1):22-28. [doi: 10.1002/ncp.10588] [Medline: 33125793]
47. Soeters PB, Wolfe RR, Shenkin A. Hypoalbuminemia: pathogenesis and clinical significance. JPEN J Parenter Enteral Nutr. 2019;43(2):181-193. [FREE Full text] [doi: 10.1002/jpen.1451] [Medline: 30288759]
48. Güven B, Can M. Fibrinogen: structure, abnormalities and laboratory assays. Adv Clin Chem. 2024;120:117-143. [doi: 10.1016/bs.acc.2024.03.004] [Medline: 38762239]
49. Brinkmann J, Zeißler E-C, Scharrenberg JS, Schenk J, Majjouti M, Oberste M, et al. The diagnostic value of cytokines for the discrimination of vertebral osteomyelitis and degenerative diseases of the spine. Cytokine. 2022;150:155782. [FREE Full text] [doi: 10.1016/j.cyto.2021.155782] [Medline: 34933239]
50. Vandenbroucke JP, von Elm E, Altman DG, Gøtzsche PC, Mulrow CD, Pocock SJ, et al. STROBE Initiative. Strengthening the Reporting of Observational Studies in Epidemiology (STROBE): explanation and elaboration. PLoS Med. 2007;4(10):e297. [FREE Full text] [doi: 10.1371/journal.pmed.0040297] [Medline: 17941715]
51. Riley RD, Collins GS. Stability of clinical prediction models developed using statistical or machine learning methods. Biom J. 2023;65(8):e2200302. [FREE Full text] [doi: 10.1002/bimj.202200302] [Medline: 37466257]
52. Collins GS, Dhiman P, Ma J, Schlussel MM, Archer L, Van Calster B, et al. Evaluation of clinical prediction models (part 1): from development to external validation. BMJ. 2024;384:e074819. [FREE Full text] [doi: 10.1136/bmj-2023-074819] [Medline: 38191193]
53. Gosho M, Ohigashi T, Nagashima K, Ito Y, Maruo K. Bias in odds ratios from logistic regression methods with sparse data sets. J Epidemiol. 2023;33(6):265-275. [FREE Full text] [doi: 10.2188/jea.JE20210089] [Medline: 34565762]
54. Zheng Z, Luo J, Zhu Y, Du L, Lan L, Zhou X, et al. Development and validation of a dynamic real-time risk prediction model for intensive care units patients based on longitudinal irregular data: multicenter retrospective study. J Med Internet Res. 2025;27:e69293. [FREE Full text] [doi: 10.2196/69293] [Medline: 40266658]
55. Trinkley KE, Simon ST, Rosenberg MA. Impact of an alert-based inpatient clinical decision support tool to prevent drug-induced long QT syndrome: large-scale, system-wide observational study. J Med Internet Res. 2025;27:e68256. [FREE Full text] [doi: 10.2196/68256] [Medline: 40228236]
56. Janse RJ, Stel VS, Jager KJ, Tripepi G, Zoccali C, Dekker FW, et al. When impact trials are not feasible: alternatives to study the impact of prediction models on clinical practice. Nephrol Dial Transplant. 2024;40(1):27-33. [FREE Full text] [doi: 10.1093/ndt/gfae170] [Medline: 39020254]
57. Berbari EF, Kanj SS, Kowalski TJ, Darouiche RO, Widmer AF, Schmitt SK, et al. Executive summary: 2015 Infectious Diseases Society of America (IDSA) clinical practice guidelines for the diagnosis and treatment of native vertebral osteomyelitis in adults. Clin Infect Dis. 2015;61(6):859-863. [FREE Full text] [doi: 10.1093/cid/civ633] [Medline: 26316526]
58. Jehi L, Ji X, Milinovich A, Erzurum S, Rubin BP, Gordon S, et al. Individualizing risk prediction for positive coronavirus disease 2019 testing: results from 11,672 patients. Chest. 2020;158(4):1364-1375. [FREE Full text] [doi: 10.1016/j.chest.2020.05.580] [Medline: 32533957]

XSL•FO
RenderX

Abbreviations

AUC: area under the receiver operating characteristic curve
CIC: clinical impact curve
CT: computed tomography
DCA: decision curve analysis
DXA: dual-energy X-ray absorptiometry
EPP: events per predictor parameter
GVIF: generalized variance inflation factor
IL-6: interleukin-6
ISCD: International Society for Clinical Densitometry
LASSO: least absolute shrinkage and selection operator
MCAR: missing completely at random
MRI: magnetic resonance imaging
MRSA: methicillin-resistant Staphylococcus aureus
OR: odds ratio
RCS: restricted cubic spline
ROC: receiver operating characteristic
TRIPOD: Transparent Reporting of a Multivariable Prediction Model for Individual Prognosis or Diagnosis

Edited by S Brini; submitted 11.Feb.2026; peer-reviewed by Y Han, LTO Cornejo, M Liu; comments to author 18.Sep.2026; revised version received 23.Oct.2026; accepted 08.Nov.2026; published 26.Nov.2026

Please cite as:
Chen X, Kuang S, Dang R, Li Y, Wang G, Sun J, Zhou F, Tan H, Zhang C
Integrating Multidimensional Clinical Data to Develop a Visual Nomogram for Individualized Prediction of Postinfectious Bone Loss in Patients With Spinal Infection: Retrospective Cohort Study
J Med Internet Res 2026;28:e93326
URL: https://www.jmir.org/2026/1/e93326
doi: 10.2196/93326
PMID:

©Xi Chen, Shouxiang Kuang, Rongpan Dang, Yang Li, Guodong Wang, Jianmin Sun, Fengge Zhou, Hongdong Tan, Chenggui Zhang. Originally published in the Journal of Medical Internet Research (https://www.jmir.org), 26.Nov.2026. This is an open-access article distributed under the terms of the Creative Commons Attribution License (https://creativecommons.org/licenses/by/4.0/), which permits unrestricted use, distribution, and reproduction in any medium, provided the original work, first published in the Journal of Medical Internet Research (ISSN 1438-8871), is properly cited. The complete bibliographic information, a link to the original publication on https://www.jmir.org/, as well as this copyright and license information must be included.

XSL•FO
RenderX